the earliest step of replication initiation (*1*, *2*), FFA-1 is likely to be a factor involved in the establishment of functional origin complexes within nuclei. The purification of quantities of FFA-1 able to be sequenced should allow for a direct molecular dissection of its role in foci formation. Moreover, the in vitro system and the assay procedures used for purification of FFA-1 should facilitate the purification of the remaining factors required for the assembly of foci. Purification of these factors will provide a biochemically tractable system for understanding how the spatial aggregation of DNA into discrete, intranuclear domains participates in the initiation of DNA replication, in particular, and in DNA function, in general, in eukaryotic cells.

REFERENCES AND NOTES

1. B. Stillman, *Annu. Rev. Cell Biol.* **5**, 197 (1989).
2. S. Waga and B. Stillman, *Nature* **369**, 207 (1994).
3. J. Newport, *Cell* **48**, 205 (1987).
4. M. A. Sheehan, A. D. Mills, A. M. Sleeman, R. A. Laskey, J. J. Blow, *J. Cell Biol.* **106**, 1 (1988).
5. H. Nakamura, T. Morita, C. Sato, *Exp. Cell Res.* **165**, 291 (1986).
6. H. Nakayasu and R. Berezney, *J. Cell Biol.* **108**, 1 (1989).
7. A. D. Mills *et al.*, *J. Cell Sci.* **94**, 471 (1989).
8. L. S. Cox and R. A. Laskey, *Cell* **66**, 271 (1991).
9. Y. Adachi and U. K. Laemmli, *J. Cell Biol.* **119**, 1 (1992).
10. ———, *EMBO J.* **13**, 4153 (1994).
11. H. Yan and J. Newport, *J. Cell Biol.* **129**, 1 (1995).
12. C. Smythe and J. W. Newport, *Methods Cell Biol.* **35**, 449 (1991).
13. Cytosol from unfertilized *Xenopus* eggs was diluted two times with ELB [250 mM sucrose, 2.5 mM $MgCl_2$, 50 mM KCl, 1 mM dithiothreitol (DTT), and 10 mM Hepes (pH 7.7)] and precipitated with AS at the following saturations: 37.5% (AS fraction 1), 37.5 to 52.5% (AS fraction 2), and 52.5 to 75% (AS fraction 3). These fractions were resuspended in ELB (1/4 of the starting cytosol volume) and dialyzed extensively against ELB. The standard RP-A foci formation cocktail contains 2 μl of AS fraction 3, 1 μl of 10× ATP regeneration system (20 mM ATP, 200 mM phosphocreatine, 50 μg/ml creatine phosphokinase, and 20 mM $MgCl_2$), 120 nM RP-A (*20*), and 500 μl of sperm with membranes removed. The fraction to be assayed and ELB were then added to the cocktail to make a final volume of 10 μl. After 60 min at room temperature, sperm were fixed and stained for RP-A with an RP-A antibody and for DNA with bisbenzimide as described (*11*).
14. H. Yan and J. Newport, unpublished data.
15. ———, unpublished data.
16. M. Benedetti, I. Baldi, E. Mottoccia, G. P. Tocchini-Valentini, *EMBO J.* **2**, 1303 (1983).
17. M. Shioda, E. M. Nelson, M. L. Bayne, R. M. Benbow, *Proc. Natl. Acad. Sci. U.S.A.* **79**, 7209 (1982).
18. H. Yan and J. Newport, unpublished data.
19. S. P. Bell and B. Stillman, *Nature* **357**, 128 (1992).
20. F. Fang and J. W. Newport, *J. Cell Sci.* **106**, 983 (1993).
21. H. Yan and J. Newport, unpublished data.
22. The FFA-1 protein was purified by the following procedure (performed at 4°C). AS fraction 1 from 50 ml of cytosol was resuspended in buffer A [25 mM tris·HCl (pH 7.5), 1 mM EDTA, and 1 mM DTT] supplemented with 1 μg of aprotinin per milliliter and leupeptin. After dialysis against the same buffer, the sample was adjusted to an NaCl concentration of 200 mM and then loaded onto a ssDNA cellulose column (1 cm by 8 cm; Amersham) equilibrated with buffer A200 (buffer A plus 200 mM NaCl). The column was washed with A250 (buffer A plus 250 mM NaCl) and eluted with A600 (buffer A plus 600 mM NaCl). The A600 fraction was adjusted to an NaCl concentration of 50 mM with A0 and applied to a HiTrap heparin column (2 ml; Pharmacia), which was then eluted with a 24-ml linear gradient of NaCl (50 to 650 mM) in buffer A. The active fractions (around 450 mM) were pooled, adjusted to an NaCl concentration of 100 mM with A0, and loaded onto a Mono Q column (1 ml; Pharmacia). Bound proteins were eluted with a 16-ml linear gradient of NaCl (100 to 500 mM) in buffer A; FFA-1 eluted around 300 mM. This procedure yielded about 10 μg of FFA-1, with a yield of about 20%.
23. B. R. Oakley, D. R. Kirsch, N. R. Morris, *Anal. Biochem.* **105**, 361 (1980).

24. This work was supported by NIH grant GM33523 to J.N.

5 June 1995; accepted 7 August 1995

Inhibition of ICE Family Proteases by Baculovirus Antiapoptotic Protein p35

Nancy J. Bump, Maria Hackett, Margaret Hugunin, Somasekar Seshagiri, Kenneth Brady, Patrick Chen, Catherine Ferenz, Simon Franklin, Tariq Ghayur, Ping Li, Peter Licari, John Mankovich, Lianfa Shi, Arnold H. Greenberg, Lois K. Miller, Winnie W. Wong*

The baculovirus antiapoptotic protein p35 inhibited the proteolytic activity of human interleukin-1β converting enzyme (ICE) and three of its homologs in enzymatic assays. Coexpression of p35 prevented the autoproteolytic activation of ICE from its precursor form and blocked ICE-induced apoptosis. Inhibition of enzymatic activity correlated with the cleavage of p35 and the formation of a stable ICE-p35 complex. The ability of p35 to block apoptosis in different pathways and in distantly related organisms suggests a central and conserved role for ICE-like proteases in the induction of apoptosis.

Apoptosis (programmed cell death) is essential for normal development and homeostasis in multicellular organisms and provides a defense against viral invasion and oncogenesis (*1*). The *p35* gene from *Autographa californica* nuclear polyhedrosis virus (AcMNPV) encodes an inhibitor that blocks apoptosis in mammalian and insect cell lines (*2*–*3*) and in developing embryos and eyes of transgenic *Drosophila melanogaster* (*4*) and partially substitutes for *ced*-9 function in *Caenorhabditis elegans* (*5*). The ability of p35 to block apoptosis induced by different signals in diverse organisms suggests that it acts at a central and phylogenetically conserved point in the apoptotic pathway. The mechanism by which p35 blocks apoptosis is not known, but it may be an inhibitor of the proteases of the ICE family. The involvement of these proteases in apoptosis was suggested when ICE or the related proteins ICE–CED-3 homolog-1 (ICH-1), ICH-2, or CPP32 induced cell death when each was overexpressed in mammalian or insect cell lines (*6*–*9*). However, because ICE-deficient mice do not exhibit the hallmarks of defective apoptosis, the apoptotic process may require the involvement of more than one member of the *ICE* gene family (*10*).

We tested the ability of p35 to inhibit ICE activity in a COS-1–derived cell line that constitutively expressed human prointerleukin-1β (proIL-1β) (*11*). Cotransfection of these cells with increasing amounts of plasmids encoding p35 and encoding either the p45 form (residues 1 to 404) or the p32 form (residues 120 to 404) of ICE resulted in decreases of as much as 90% in the release of mature IL-1β (Fig. 1A). To control for the possibility that p35 interfered with the expression of ICE or proIL-1β, we immunoprecipitated these proteins and showed that the amounts of p32 ICE precursor and proIL-1β were similar in the presence or absence of p35 (*12*). These findings suggest that p35 inhibits the enzymatic activity of ICE.

To confirm more directly that p35 is an ICE inhibitor, we purified recombinant p35 and tested it in a colorimetric assay that measured the activity of purified recombinant human ICE on a tetrapeptide substrate. In addition, we tested p35 with three other purified recombinant human ICE homologs, ICH-1, ICH-2, and CPP32 (*13*, *14*). Cleavage of the respective tetrapeptide substrates by ICE, ICH-1, ICH-2, and CPP32 was inhibited in a concentration-dependent manner when the enzymes were

N. J. Bump, M. Hackett, M. Hugunin, K. Brady, P. Chen, C. Ferenz, S. Franklin, T. Ghayur, P. Li, P. Licari, J. Mankovich, W. W. Wong, BASF Bioresearch Corporation, 100 Research Drive, Worcester, MA 01605, USA.
S. Seshagiri and L. K. Miller, Departments of Entomology and Genetics, University of Georgia, Athens, GA 30602, USA.
L. Shi and A. H. Greenberg, Manitoba Institute of Cell Biology, University of Manitoba, Winnipeg, Manitoba R3E 0V9, Canada.

*To whom correspondence should be addressed.

first preincubated with p35. Maximal inhibition was achieved in each case at approximately equimolar amounts of p35 and the protease (Fig. 1B). Purified p35 had no effect on the proteolytic activity of granzyme B, a serine protease with similar preference for aspartic acid at the P1 site of its substrates (*15*).

When the reaction mixtures that contained varying ratios of p35 and ICE were analyzed by SDS–polyacrylamide gel electrophoresis (PAGE) and immunoblotting (*16*), p35 was completely cleaved to a 25-kD fragment in the presence of excess ICE. When p35 was in excess, ICE-mediated cleavage of p35 reached a maximum that corresponded to the total amount of inhibited enzyme (Fig. 1C). The apparent lack of substrate turnover suggested that p35 is an irreversible inhibitor rather than a competitive substrate for the protease. A similar pattern of p35 cleavage was obtained with ICH-2 (*17*).

We confirmed that p35 acts as an irreversible, or very slowly reversible, inhibitor by isolating a complex of ICE and the cleavage fragments of p35. To isolate this complex, we prepared ^{35}S-labeled p35 protein and reacted it with excess amounts of ICE. Because ICE is a homodimer (*18*) and because inhibition by p35 is stoichiometric, isolation of an ICE-p35 complex by active-site ligand-affinity chromatography is possible when excess enzyme is present. The p35 cleavage fragments copurified with the enzyme upon addition of a biotinylated tetrapeptide aldehyde, Ac-Tyr-Val-Lys(biotin)-Asp-aldehyde [AcYVK(biotin)D-CHO], and streptavidin-agarose (*19*, *20*). When p35 was mixed with ICE that had been completely inhibited with the tetrapeptide aldehyde, no p35 cleavage was observed and the intact p35 did not copurify with ICE. In the absence of the affinity ligand, p35 did not bind to streptavidin-agarose (Fig. 2A). Although radiolabeled human proIL-1β was efficiently cleaved upon incubation with ICE, no detectable cleavage products of this natural substrate copurified with the enzyme (*21*). We conclude that cleavage by ICE is necessary and sufficient for the formation of the ICE-p35 complex and that a stable interaction is not a property of ICE with its natural substrate, proIL-1β.

Stable complexes of ICE and p35 were found in culture media of *Spodoptera frugiperda* SF-9 cells infected with recombinant

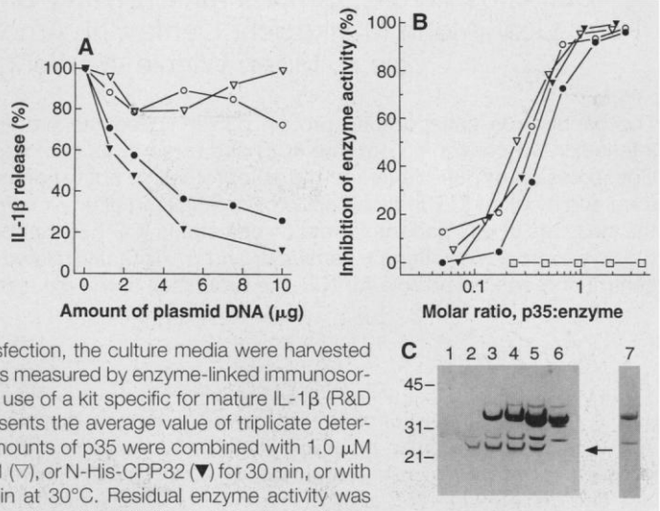

Fig. 1. Functional inhibition of ICE family proteases by AcMNPV p35. (**A**) COS cells that constitutively expressed proIL-1β were cotransfected with 7.5 μg of plasmid encoding the p45 form (▽ and ▼) or the p32 form (○ and ●) of ICE and increasing amounts of pkV vector alone (○ and ▽) or plasmid encoding p35 (● and ▼) (*11*). At 24 hours after transfection, the culture media were harvested and the amount of IL-1β was measured by enzyme-linked immunosorbent assay (ELISA) with the use of a kit specific for mature IL-1β (R&D Systems). Each point represents the average value of triplicate determinations. (**B**) Increasing amounts of p35 were combined with 1.0 μM purified ICE (○), N-His-ICH-1 (▽), or N-His-CPP32 (▼) for 30 min, or with N-His-ICH-2 (●) for 120 min at 30°C. Residual enzyme activity was measured with tetrapeptide *p*-nitroanilide (pNA) substrates in colorimetric assays (*14*). Each point represents the average value of triplicate samples. Granzyme B assays (□) were performed with 10 nM protease and *tert*-butyloxycarbonyl-Ala-Ala-Asp-thiobenzyl ester as substrate (*15*). (**C**) Reaction mixtures containing 1.0 μM ICE and 0, 0.3, 0.9, 2.8, or 8.3 μM p35 (lanes 1 to 5, respectively) were incubated in assay buffer at 30°C for 30 min and analyzed by SDS-PAGE and immunoblotting with anti-p35 (*16*). The NH_2-terminus of p35 is not recognized by the anti-p35 used in these studies. Lane 6 contains 0.6 μg of p35 alone; lane 7 represents the Coomassie blue–stained gel of purified p35 used in all the experiments. Molecular masses are indicated in kilodaltons; the arrow on the right designates the 25-kD cleavage product of p35.

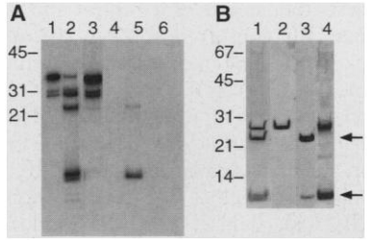

Fig. 2. Association of ICE with the cleavage products of p35. (**A**) ^{35}S-labeled p35 was incubated alone (lane 1), with ICE (lanes 2, 5, and 6), or with enzyme that had been inhibited with AcYVK(biotin)D-CHO (lanes 3 and 4). After incubation at 30°C for 30 min, AcYVK(biotin)D-CHO was added to the sample in lane 5, followed by addition of streptavidin-agarose (lanes 4 to 6). The beads were washed extensively and the eluted proteins were analyzed by SDS-PAGE and autoradiography (*19*). The NH_2-terminal portion of p35 includes five methionines, and the darker bands at 10 and 11 kD probably represent two alternate cleavage products derived from the NH_2-terminus. The residual band at 35 kD (lane 2) may represent an alternate translation product because it was not cleaved by a large molar excess of ICE. The doublet at 30 kD was observed only with the addition of DNA encoding p35 and probably represents translation products that either started at internal methionines or stopped prematurely. (**B**) SDS-PAGE and immunoblot analysis of ICE-p35 complex purified from SF-9 cell cultures. The ICE-p35 complex was purified by affinity chromatography (lanes 1 to 3) (*23*) and analyzed by SDS-PAGE. After electrophoresis, proteins were transferred to nitrocellulose membranes (lanes 2 and 3) and the blots were incubated with anti-p35 (lane 2) or with anti-p20 and anti-p10 ICE (lane 3) visualized by enhanced chemiluminescence. The arrows on the right denote the positions of the native p20 and p10 subunits of ICE. Similar results were obtained when N-His-ICE–p35 was purified by IMAC (lane 4) (*24*). In the preparation of N-His-ICE, the 25-kD fragment of p35 comigrated with the N-His-p20 subunit of ICE in these gels (lane 4). The proteins in lanes 1 and 4 were developed by silver staining.

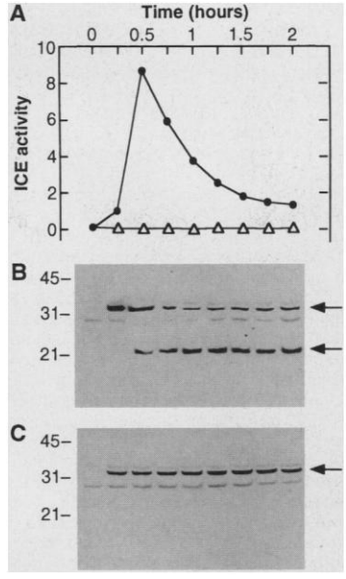

Fig. 3. Profile of ICE activity and ICE protein in *E. coli* after heat induction. (**A**) *Escherichia coli* that expressed the p32 form of ICE alone (●) or bicistronically with p35 (△) under the control of the λ pL promoter were induced at 40°C (*28*). Cells (25 ml) were removed at the time intervals shown; these aliquots were lysed and the clarified lysates were saved for measurement of ICE activity. ICE activity was measured in a colorimetric assay with AcYVAD-pNA as substrate and is expressed in relative absorbance units. (**B** and **C**) Immunoblot analysis of expression of the p32 form of ICE alone (B) or bicistronically with p35 (C). SDS-PAGE and immunoblot analysis with anti-p20 ICE and enhanced chemiluminescence were performed on 10-μl aliquots of the lysates removed at the time intervals shown in (A). The arrows on the right denote the positions of the p32 form (B and C) and the p20 form (B) of ICE.

viruses expressing either the p45 or p32 form of ICE (*22*). A typical complex isolated by sequential cation exchange and ligand-affinity chromatography with the use of AcYVK-(biotin)D-CHO and streptavidin-agarose (*23*) contained four bands that migrated at 25, 22, 11, and 10 kD (Fig. 2B). Immunoblotting with antibodies to ICE showed that the 22-kD and 10-kD bands corresponded to the p20 (residues 120 to 297) and p10 (residues 317 to 404) subunits of ICE, respectively. We showed that the 25-kD protein was derived from p35 by immunoblotting with antibody to p35 (anti-p35) (Fig. 2B). A similar complex of ICE and p35 was obtained when we purified enzyme with a polyhistidine fusion tag at the NH_2-terminus (N-His-ICE) by immobilized metal affinity chromatography (IMAC) (Fig. 2B) (*24*). Sequence analysis showed that the NH_2-terminus of the 25-kD polypeptide started with the sequence Gly-Phe-His-Asp-Ser-Ile-Lys-Tyr-Phe-Lys-Asp-Glu-His, corresponding to residues 88 to 100 of p35 (*25*). In the intact p35 sequence, Gly^{88} is preceded by Asp^{87}, a likely site for cleavage by ICE. The NH_2-terminus of the 11-kD band was blocked, but the sequences of internal tryptic fragments showed that this band was derived from the NH_2-terminal portion of p35 (*26*).

Activation of ICE requires the proteolytic removal of an NH_2-terminal prodomain as well as the amino acids that connect the p20 and p10 subunits (*27*). To determine whether p35 could inhibit the activation of ICE, we coexpressed the proteins in *Escherichia coli* by inserting the p35 gene upstream of the DNA sequence of p32 ICE in an expression vector plasmid (*28*). Bacteria transformed with this plasmid had no ICE activity in the soluble fraction of cell lysates upon induction, and only the p32 form of ICE was detected in cell lysates. In the control lysates that contained only ICE, protease activity was readily detectable 30 min after heat induction and correlated with the appearance of the p20 subunit (Fig. 3). Thus, the presence of p35 may block autoactivation of ICE in vivo and may effectively prevent ICE-like proteases from initiating apoptosis.

Infection of insect cells with baculovirus vectors that expressed ICE, ICH-2, or CPP32 under the control of the polyhedrin promoter induced apoptosis despite the presence of p35 in these systems (*8*, *10*). Such results would be expected because p35 is a stoichiometric inhibitor of ICE-like proteases. When quantities of virally encoded p35 are insufficient to block all of the recombinant ICE-like enzymes, apoptosis should proceed. When we introduced ICE into SF-9 cells through the viral vector and the protease was overexpressed under the control of the polyhedrin promoter, even the amount of p35 produced under the control of the *Drosophila Hsp70* promoter from a separate plasmid was insufficient to block ICE-mediated cell death (Table 1).

An effective blockade of ICE-induced apoptosis in insect cells would require expression of p35 at amounts comparable to that of ICE. To achieve this, we cotransfected SF-21 cells with plasmids encoding p35 or ICE (*29*). In the presence of p35, apoptosis was reduced by 81% and 45% with and without heat shock, respectively (Table 1). Cell death was associated with the formation of apoptotic bodies and resulted in the degradation of chromosomal DNA, which gave rise to oligonucleosomal ladder patterns (*30*). Apoptosis could also be induced by transient expression of ICE in *Trichoplusia ni* TN-368 (Table 1), an insect cell line that is more resistant to apoptosis (*2*). Cotransfection with p35 resulted in an 85% reduction in apoptosis. These results support the hypothesis that the antiapoptotic effects of p35 are mediated through the inhibition of ICE-like proteases.

The involvement of a proteolytic activation mechanism at a critical point in pathways that lead to apoptosis obviates the requirement for gene expression. The protease inhibitor p35 has no apparent homologs in available databases and no obvious sequence motifs that suggest a relation to other known protease inhibitors. The cleavage fragments of p35 remain associated with its target protease, reminiscent of the behavior of cytokine response modifier (crmA), the cowpox inhibitor of ICE and granzyme B (*31*). Unlike crmA, p35 has broader specificity for the ICE-like cysteine proteases but has no effect on granzyme B. The different profile of inhibition of these two viral inhibitors will help to delineate the cascade of proteolytic events required for apoptosis. The identification of potential homologs of p35 or crmA will enhance our understanding of the regulation of life-versus-death decisions in mammalian cells.

Table 1. Baculovirus p35 blocks apoptosis induced by expression of ICE in insect cells. ICE was introduced through a recombinant virus (BV-ICE) (*22*) into SF-9 cells at a multiplicity of infection of 5 after initial transfection of the cells with pHSP35VI$^+$ (p35). In separate experiments, plasmids pHSPICE32VI$^+$ (ICE) and pHSP35VI$^+$ (p35) or pBluescript KS$^+$ (BS) were transfected into either SF-21 or TN-368 cells. At 20 hours after transfection, cells were either maintained at 27°C or heat-shocked (*29*); HS indicates heat shock. Where possible, viable cells indicated by exclusion of trypan blue were counted at 30 to 32 hours after transfection; ND indicates that there were too few viable cells to be counted. The total number of cells counted and the mean number of cells counted per grid (±SEM) are shown.

ICE (μg)	p35 (μg)	BS (μg)	HS	Viable cells		Apoptosis (%)
				Total	Per grid	
SF-9 cells plus BV-ICE						
0	2.0	0	+	ND	ND	>95
0	2.0	0	−	ND	ND	>95
0	0	0	+	ND	ND	>95
0	0	0	−	ND	ND	>95
SF-21 cells						
0.5	0	0.5	+	261	21.8 ± 0.0	74
0.5	0	0.5	−	531	44.4 ± 0.1	47
0.5	0.5	0	+	855	71.4 ± 3.3	14
0.5	0.5	0	−	773	64.4 ± 3.6	26
0	0	1.0	+	1002	83.3 ± 5.1	0
TN-368 cells						
5.0	0	5.0	+	1035	86.3 ± 4.8	34
5.0	5.0	0	+	1494	124.5 ± 4.8	5
0	0	10.0	+	1568	130.7 ± 5.4	0

REFERENCES AND NOTES

1. H. Steller, *Science* **267**, 1445 (1995); C. B. Thompson, *ibid.*, p. 1456.
2. R. J. Clem, M. Fechheimer, L. K. Miller, *ibid.* **254**, 1388 (1991); R. J. Clem and L. K. Miller, *Mol. Cell. Biol.* **14**, 5212 (1994).
3. S. Rabizadeh, C. D. La, P. D. Friesen, D. E. Bredesen, *J. Neurochem.* **61**, 2318 (1993); J. L. Cartier, P. A. Hershberger, P. F. Friesen, *J. Virol.* **68**, 7728 (1994).
4. B. A. Hay, T. Wolff, G. M. Rubin, *Development* **120**, 2121 (1994).
5. A. Sugimoto, P. D. Friesen, J. H. Rothman, *EMBO J.* **13**, 2023 (1994).
6. M. Miura, H. Zhu, R. Rotello, E. A. Hartwieg, J. Yuan, *Cell* **75**, 653 (1993).
7. L. Wang, M. Miura, L. Bergeron, H. Zhu, J. Y. Yuan, *ibid.* **78**, 739 (1994); S. Kumar, M. Kinoshita, M. Noda, N. G. Copeland, N. A. Jenkins, *Genes Dev.* **8**, 1613 (1994).
8. T. Fernandes-Alnemri, G. Litwack, E. S. Alnemri, *J. Biol. Chem.* **269**, 30761 (1994); M. Tewari *et al.*, *Cell* **81**, 801 (1995); D. W. Nicholson *et al.*, *Nature* **376**, 37 (1995).
9. J. Kamens *et al.*, *J. Biol. Chem.* **270**, 15250 (1995); C. Faucheu *et al.*, *EMBO J.* **14**, 1914 (1995).
10. P. Li *et al.*, *Cell* **80**, 401 (1995); K. Kuida *et al.*, *Science* **267**, 2000 (1995).
11. COS cells that constitutively produced human proIL-1β were generated by transfection with DNA encoding this sequence in the MNC(neo) vector. Cells that contained stably integrated DNA were enriched by selection in media that contained G418. The coding sequences for p45 ICE, p32 ICE, and p35 were subcloned into modified pSVb vector (pkV) (Clontech) under the control of the SV40 promoter. The cells were plated at 3×10^6 cells per 100-mm dish and were transfected by the DEAE-dextran method.
12. For immunoprecipitations, COS cells that expressed both the p32 and p35 forms of ICE were labeled with 200 μCi/ml of translation-grade [^{35}S]methionine (1150 Ci/mmol, NEN-DuPont), washed, and lysed.

The cell lysates were incubated sequentially with preimmune sera, polyclonal rabbit antibodies to human IL-1β, or anti-p20 ICE and protein A–agarose. After extensive washes, the adsorbed proteins were eluted by boiling the beads in SDS-PAGE sample buffer and analyzed by SDS-PAGE and autoradiography.

13. The ICE homologs and p35 were expressed in *E. coli* under the control of the λ pL promoter. ICH-1 (*7*) and CPP32α (*8*) contained a polyhistidine linker and were purified by IMAC as described for ICH-2; p35 was purified by chromatography on Q-Sepharose, Mono-Q, and Superdex-75.
14. Colorimetric assays were performed in 96-well plates by incubating enzyme in assay buffer [100 mM Hepes (pH 7.5), 0.5 mM EDTA, 20% glycerol, and 5 mM dithiothreitol] with *N*-acetyl-Tyr-Val-Ala-Asp-*p*-nitroanilide (AcYVAD-pNA) as substrate for ICE and ICH-2 or with *N*-acetyl-Asp-Glu-Val-Asp-*p*-nitroanilide (AcDEVD-pNA) (Quality Controlled Biochemicals, Hopkinton, MA) as substrate for ICH-1 and CPP32. Absorbance at 405 nm was monitored at 37°C for 30 min.
15. L. Shi, C. M. Kam, J. C. Powers, R. Aebersold, A. H. Greenberg, *J. Exp. Med.* **176**, 1521 (1992).
16. Proteins were separated on gels containing a 10 to 20% gradient of acrylamide (Integrated Separations Science, Natick, MA) in tris-tricine buffer under reducing conditions. For immunoblot analysis, the proteins were electrophoretically transferred onto nitrocellulose and the membranes were blocked, washed, and incubated in purified rabbit immunoglobulin G (IgG) followed by donkey antibodies to horseradish peroxidase–conjugated rabbit IgG (Amersham). Immunoblots were developed by enhanced chemiluminescence (Amersham). Rabbit antisera to p35 were produced against residues 75 to 299 fused to trpE of *E. coli*. ICE has a k_{cat} value of 0.5 mol aminomethylcoumarin (Amc) mol^{-1} s^{-1} compared to 1 mol Amc mol^{-1} s^{-1} reported previously (*27*). When approximately equal amounts of ICE and p35 protein were used, only about half of the p35 was cleaved (Fig. 2B, lane 3), consistent with the presence of some inactive enzyme in the preparations used.
17. N. Bump, unpublished results.
18. N. P. C. Walker *et al., Cell* **78**, 343 (1994); K. P. Wilson *et al., Nature* **370**, 270 (1994).
19. DNAs encoding p35 or human proIL-1β were subcloned into pSVb. The TNT T7-coupled reticulocyte system (Promega) was used to generate proteins labeled with [^{35}S]methionine (15 mCi/ml, Amersham). Radiolabeled p35 was incubated with ICE at 30°C for 30 min, and the reactions were stopped by heating in SDS-PAGE sample buffer. For the reassociation experiments, the mixtures that contained ICE, AcYVK(biotin)D-CHO, and ^{35}S-labeled p35 or human proIL-1β were incubated with streptavidin-agarose. The beads were washed, adsorbed proteins were eluted by boiling in 1% SDS, and the labeled proteins were detected by autoradiography after SDS-PAGE.
20. Equimolar amounts of *N*-acetyl-Tyr-Val-Lys-Asp-aldehyde (Bachem Bioscience) and (biotinoyl-ε-aminocaproyl)-ε-aminocaproic acid *N*-hydroxysuccinimide ester (Molecular Probes) were combined in a 1:1 mixture of ethanol and 100 mM sodium borate (pH 8.5) for 80 min at room temperature. The biotinylated product was separated from the starting peptidyl aldehyde by reversed-phase high-performance liquid chromatography (HPLC). The biotinylated peptide aldehyde AcYVK(biotin)D-CHO inhibited ICE with a K_i of less than 1 nM.
21. N. Bump, unpublished results.
22. Complementary DNA fragments encoding either the p32 or p45 forms of human ICE were inserted into pVL1393 (Invitrogen). The transfer plasmid was cotransfected into SF-9 cells with linearized AcMNPV DNA by means of the BaculoGold system (Pharmingen). Recombinant virus expressing ICE (BV-ICE) was purified by several rounds of infection.
23. For production of ICE, SF-9 cells were infected at a multiplicity of infection of 2 to 5 with recombinant virus stock with a titer of 1×10^8 plaque-forming units per milliliter. The medium was harvested when cell viability was between 0 and 20% and concentrated on SP-Sepharose HP (Pharmacia). We added 10 mM dithiothreitol, 3 mM AcYVK(biotin)D-CHO, and streptavidin-agarose to the eluted protein. Affinity-purified enzyme was eluted by addition of 100 mM Hepes, 20% glycerol, 100 mM hydroxylamine, 10 mM oxidized glutathione (GSSG), and 0.5 mM EDTA (pH 7.5).
24. We introduced six histidine residues at the NH_2-terminus of p32 ICE with the use of a Lys-Ser-Gly-Ala-Asp-Asp-Asp-Asp-Asp-Lys linker and produced recombinant virus expressing this construct (N-His-ICE) as described (*22*). Culture medium from SF-9 cells infected with this virus was loaded onto HiTrap Chelating Sepharose (Pharmacia) charged with $NiCl_2$, and the N-His-ICE–p35 complex was eluted by addition of 150 mM imidazole.
25. Proteins were separated by SDS-PAGE on 14% acrylamide gels and transferred onto ProBlott (Applied Biosystems). After detection by Ponceau-S staining, the bands of interest were excised and NH_2-terminal sequencing was performed.
26. C. Ferenz, unpublished results. Proteins were transferred onto nitrocellulose membrane and digested with trypsin (Promega). The tryptic peptides were separated by reversed-phase HPLC and sequenced on an Applied Biosystems 477A pulse-liquid phase automated sequencer.
27. N. A. Thornberry *et al., Nature* **356**, 768 (1992).
28. Complementary DNA encoding the p32 form of ICE was subcloned into a pBluescript II KS$^+$ (Stratagene) derivative under the control of the bacteriophage λ pL promoter. We constructed a second plasmid with the p35 gene inserted upstream of the ICE gene, thus creating a bicistronic message for coexpression in *E. coli* mm294 cells. Cells were grown at 29°C to an optical density of 0.6 at 600 nm and were induced to synthesize recombinant proteins by raising the temperature to 40°C.
29. The plasmid pHSP35VI$^+$ contains p35 under the control of the *Drosophila Hsp70* promoter in a pBluescript-based (Stratagene) plasmid vector (*2*). This promoter is constitutively transcribed upon transfection in SF-21 cells and can be stimulated further by heat shock (*2, 32*). Plasmid pHSPICE32VI$^+$ is identical to pHSP35VI$^+$ except that it contains p32 ICE instead of p35. SF-21 cells or TN-368 cells (5×10^5 to 6×10^5 per 35-mm dish) were transfected with plasmid DNA with the use of Lipofectin (Bethesda Research Laboratories). At 20 hours posttransfection, cells were heat-shocked for 30 min at 42°C. The media were removed 10 to 12 hours after heat shock, the cells were resuspended in 500 μl of phosphate-buffered saline containing 0.04% trypan blue, and viable cells were counted with a hemocytometer. Transfections were repeated in triplicate and viable cells in four grids of the hemocytometer were counted for each replicate.
30. S. Seshagiri, unpublished results. SF-21 or TN-368 cells were transfected with pBluescript, pHSPICE32VI$^+$, and pHSP35VI$^+$ and total DNA was isolated, electrophoresed through an agarose gel, and visualized by ethidium bromide staining.
31. C. A. Ray *et al., Cell* **69**, 597 (1992); L. T. Quan, A. Caputo, R. C. Bleackley, D. J. Pickup, G. S. Salvesen, *J. Biol. Chem.* **270**, 10377 (1995).
32. T. D. Morris and L. K. Miller, *J. Virol.* **66**, 7397 (1992).

33. We thank L. Perron for manuscript preparation and B. Seed of Harvard Medical School for the MNC(neo) vector. Supported in part by U.S. Public Health Service grant AI 38262 to L.K.M.

16 May 1995; accepted 4 August 1995

TECHNICAL COMMENTS

Honeybees and Magnetoreception

Chin-Yuan Hsu and Chia-Wei Li (*1*) propose that magnetite particles in the fat body of honeybees are part of a magnetic field sensory system used for navigation. They make the following statements that we think are in error or may have other interpretations.

1) Honeybees contain iron in "granules" only in the fat body. Iron granules have been described in honeybee midgut as well as the fat body (*2*). They are mineral concretions in vacuoles derived from the rough endoplasmic reticulum (RER) and form in response to iron in pollen in the diet.

2) Iron in honeybee fat body occurs in particles 7.5 nm in diameter. We have identified iron in holoferritin in the RER of many insects. Holoferritin has dense cores 7.5 nm in diameter (*3, 4*), the size of the particles mentioned by Hsu and Li. The dense masses in the iron granules look like hemosiderin degradation products of holoferritin described in other insects (*5*). Hsu and Li make no mention of ferritin or hemosiderin.

3) The fat body is innervated. Their scanning electron micrograph [figure 2B in (*1*)] illustrating innervation of a fat body shows a filamentous structure resembling a trachea. Hsu and Li do not mention the tracheae and tracheoles commonly observed on the surface of the fat body–oenocyte complex, or how they may be distinguished from nerves in scanning electron micrographs. Innervation of insect fat body has not been described. Should the honeybee fat body–oenocyte complex prove an exception, it may be related to the control of wax secretion rather than to magnetotaxis. The transmission electron micrograph of a nerve ending in a fat body [figure 2C in (*1*)] shows the synaptic vesicles appropriate for an excitatory nerve rather than the sensory nerve required for a magnetotactic organ.

4) Nerve endings in the fat body are stimulated through a transducer mechanism. We could find no structure corresponding to the proposed transducer complex needed to convert intracellular stress to extracellular nerve action potentials.

5) The granules are attached to cytoskeletal filaments that form the stress-activated part of the transducer complex. Honeybee vacuoles have no special attachment to cytoskeletal filaments (Fig. 1). Their bounding membranes resemble those of the rest of the RER. Preparations without osmication to preserve the cytoskeleton show filaments between mouse pancreas lamellate ER (*6*), but not around honeybee iron-containing vacuoles.

Iron concretions are abundant throughout honeybee fat body, as would be expect-